Journal of Crystal Growth 132 (1993) 377–388
North-Holland

JOURNAL OF CRYSTAL GROWTH

# Initial front transients in directional solidification of thin samples of dilute alloys

B. Caroli [1], C. Caroli and L. Ramirez-Piscina [2]

*Groupe de Physique des Solides, Université Paris 6 et Paris 7, Tour 23, 2 Place Jussieu, F-75251 Paris Cedex 05, France*

Received 15 December 1992; manuscript received in final form 11 June 1993

We study the dynamics of recoil of a planar front in a directional solidification process, following a sudden jump from rest to a constant pulling velocity $V$. To this end, we solve numerically the full integral equation describing the front dynamics in the one-sided model. We find, in particular, that the asymptotic (respectively initial) regimes, for which we derive analytical expressions for the front position, are restricted to such long (respectively short) times that they are in practice irrelevant for the analysis of experiments. We show that the results obtained from the heuristic approximation recently proposed by Warren and Langer are in remarkably good agreement with the exact ones in the regimes relevant to planar recoil experiments. Equally good agreement is found for the velocity threshold and the critical wavelength of the cellular instability after a large velocity jump, as calculated in the adiabatic approximation.

## 1. Introduction

Most recent work on directional solidification of dilute alloys has been focused on what can be called "quasi-steady" front patterns. That is, one considers situations where the transients associated with the establishment of the external constraints have died out. In practice, the external control parameter which is most easily varied in an experiment is the pulling velocity $V$, which most theoretical studies assume to have been set to its fixed value at time $t = -\infty$.

In this article, on the contrary, we concentrate on the description of the initial transient behavior. For this purpose, we will study the front behavior following instantaneous jumps from zero pulling velocity to a final constant value $V$. Two cases should be distinguished:

(i) $V < V_{MS}$, where $V_{MS}$ is the threshold of the Mullins–Sekerka (MS) [1] cellular instability of the stationary planar front (which we assume to be direct, for the sake of clarity of the present argument):

In the initial ($V = 0$) state, the liquid concentration is uniform ($C_L(z) = C_\infty$), the front is planar and settled at position $z_i$ such that $T(z_i) = T_L(C_\infty)$, where $T_L(C)$ is the liquidus curve of the binary alloy (see fig. 1). The final state is the unique stationary state at velocity $V$, it also corresponds to a planar front. However, mass conservation in the stationary state imposes that $C_S = C_\infty$, where $C_S$ is the concentration everywhere in the solid. So, on the liquid side of the front, $C_L = C_\infty/K$, where $K$ is the segregation coefficient, and $C_L(z)$ exhibits an exponential profile, with a range equal to the diffusion length $l = D/V$ ($D$ is the chemical diffusion coefficient in the liquid phase). So, the front has to move to position $z_f$ such that $T(z_f) = T_L(C_\infty/K)$ #1. In the

[1] Also at Département de Physique, Faculté des Sciences, Université de Picardie, 33 Rue Saint-Leu, F-80039 Amiens Cedex, France.

[2] Permanent address: Departament de Fisica Aplicada, Universitat Politècnica de Catalunya, Jordi Girona Salgado 31, E-08034 Barcelona, Spain.

#1 We assume that kinetic effects are negligible, as is the case for most metals in this velocity range, i.e. that there is local thermodynamic equilibrium on the front.

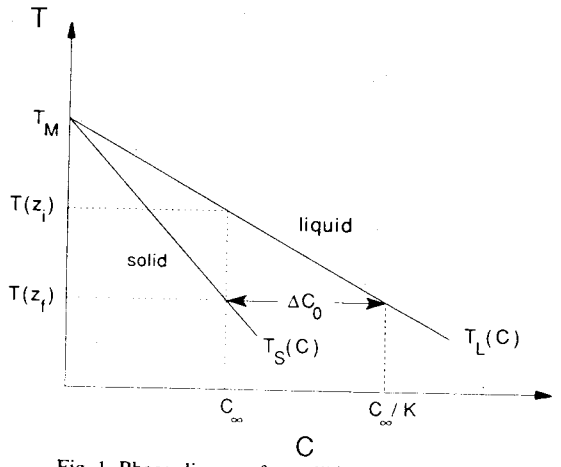


Fig. 1. Phase diagram for a dilute alloy ($K < 1$).

most common case where $K < 1$, following the velocity jump, the planar front therefore undergoes, in the laboratory frame of reference, where the temperature field is fixed, a transient recoil process.

A detailed analysis of the dynamics of this recoil is of interest in two respects:
- From the knowledge of the time dependence of the front position, one can immediately deduce the inhomogeneous concentration profile in the solid, an information of much practical interest for various technical processes, e.g. zone melting.
- Front dynamics is controlled by diffusion in the liquid. Hydrodynamic effects make accurate determinations of diffusion coefficients in liquids quite difficult. It would therefore be interesting to be able to determine $D$ from a quantitative analysis of experiments on front recoil in very thin (and therefore convection-free) samples.

(ii) $V > V_{MS}$: In this case, the complete problem of transient behavior is much more subtle and still poses unsolved basic questions. Indeed, it has been shown [2] that there exist, for given values of the external constraints, an infinite number of steady space-periodic cellular front patterns, characterized by their wavelengt' $\lambda$. Whether the system should always finally s.ect the same unique pattern or whether its final structure depends on its history is still an open question – the wavelength selection one.

We will concentrate here on a restricted problem, namely the analysis of the very first stage of the appearance of the cellular structure. Indeed, the standard Mullins–Sekerka stability analysis [1] is based on the assumption that the state on top of which cells appear is the planar stationary one. This cannot describe what effectively occurs after an instantaneous jump, taking place at $t = t_0$, from $V = 0$ to $V > V_{MS}$. Indeed, for $t = t_{0+}$, the previously immobile front starts moving into the liquid, thus solute starts piling up ahead of it. As time elapses, the front accelerates, rejection accumulates solute on its liquid side, while diffusion acts to evacuate it away into the liquid. This results in a time-dependent concentration gradient $G_c(t)$, which provides the mechanism leading to the destabilization of the planar front. If $V/V_{MS} \gg 1$, it is intuitively clear that the critical conditions for the cellular instability will be met much before the velocity of the planar front has reached its final value $V$, i.e. while the concentration profile is still non-stationary, and governed by the dynamics of the recoil transient. So, the instantaneous front velocity $v_{fr}^c$ at which instability first occurs should be different from $V_{MS}$, and should depend on the final $V$, while the wavevector $k_c$ of the first unstable cellular deformation should be different from $k_{MS}(v_{fr}^c)$ (where $k_{MS}$ has the functional dependence predicted from the MS theory).

Warren and Langer [3] have shown in their recent work on the prediction of dendritic spacings that this initial stage, where cell amplification develops on top of a recoiling front, is one of the essential steps in the selection of the fully developed directional solidification structures.

This article is organized as follows:

Sections 2 to 5 are devoted to the study of the recoil of the planar front. We write down and solve numerically the exact integro-differential equation satisfied by the front position, thus improving on the work of Clayton et al. [4], who approximated the concentration field by truncated Taylor expansions. We show, in particular, that the approximate analytic solutions of the front equation which describe the initial and asymptotic recoil regimes, although consistent with the numerical solutions, are in practice irrel-

evant for practical purposes. Indeed, the initial time expansion has an extremely narrow range of validity, while the linear asymptotic regime is reached only when the front is too close to its stationary position for the difference to be resolved in experiments.

This, we believe, explains why our results depart quite strongly from those resulting from the approximate solutions proposed by Tiller et al. [5], as well as by Smith et al. [6]. Indeed, while Tiller et al. calculate the time evolution of the interface concentration under the assumption that the concentration profile in the liquid is proportional to the final stationary one (i.e. neglect the time variation of its space range), Smith et al., who study this same quantity, assume that the front position is fixed at its final stationary value. Although their approximation improves upon that of ref. [5], the resulting approximate form of the recoil can at best be justified in the asymptotic regime.

Warren and Langer [3] have proposed an approximate solution to the planar recoil problem based on the heuristic assumption of an exponential transient concentration profile, which is therefore characterized by two time-dependent parameters, namely its amplitude and its space range $L(t)$. Mass conservation together with the condition of local equilibrium on the front then reduce the dynamical front problem to solving two coupled non-linear differential equations for the front position and $L(t)$. In the same spirit, Huang et al. [7] had proposed an approximation allowing for a time variation of a range parameter, but they assumed this to be equal to the "instantaneous diffusion length" built from the instantaneous front velocity. For this reason, their approximation cannot satisfy global mass conservation (see eq. (11) of ref. [7]).

Comparison with the results of our full numerical integration shows that the Warren–Langer (WL) approximation is extremely accurate for all practical purposes relevant to experiments – much more so indeed than we can predict on the basis of an analytical evaluation of the neglected terms.

In section 6 we calculate, within the adiabatic approximation for the linear amplification of perturbations also used by WL, the critical front velocity $V_c$ and the first unstable wave vector $k_c$ after a sudden jump of the pulling velocity from 0 to $V > V_{MS}$. We find, again, very good agreement with the WL predictions.

## 2. Model

We consider that the solidification sample is a thin one, pulled along the $(-z)$ direction in a fixed temperature gradient $G \| Oz$, with equal densities in the two phases. We assume that:
- there is no convection in the liquid;
- the thermal gradient is uniform (imposed by the confining plates);
- chemical diffusion in the solid is negligible (one sided model);
- attachment kinetics is quasi-instantaneous.

Moreover, we assume that the front is planar, which implies that we neglect meniscus-like deformations imposed by chemical equilibrium at the solid–liquid-confining plates triple contacts. Such meniscus effects may be quantitatively important [8,9], in particular when the system approaches its MS instability. However, a full calculation of recoil transients taking them into account would be extremely heavy. Moreover, the relevant contact angles are extremely difficult to measure. So, it seems reasonable, at least as a first step, to neglect this effect. A comparison of the results that we get in the fully planar approximation with systematic recoil measurements performed on samples of different thicknesses could then provide a basis for future improvements. So, the solidification process is described by the following set of equations:

(a) In the liquid phase $(z > \zeta(t))$, and in the laboratory frame:

$$\frac{\partial^2 u}{\partial z^2} + \frac{\partial u}{\partial z} = \frac{\partial u}{\partial t}. \tag{1}$$

Here, $u$ is the dimensionless concentration, $u = (C_L - C_\infty)/\Delta C_0$, where $C_\infty$ is the concentration of the solidifying liquid far ahead from the front $(u(z \to \infty, t) = 0)$;

$$\Delta C_0 = C_\infty(K^{-1} - 1) \tag{2}$$

is the equilibrium concentration gap relevant to the stationary state (see fig. 1). Lengths and times are measured in units of the diffusion length and time $l = D/V$, $\tau_D = D/V^2$ in the final stationary state where the sample is pulled at velocity $V$.

The instantaneous front position $\zeta(t)$ is measured from its stationary value (defined by $T(0) = T_L(C_\infty/K)$), so that

$$\lim_{t\to\infty} \zeta(t) = 0. \tag{3}$$

(b) On the front:

Mass conservation:

$$\partial u/\partial z \,|_{z=\zeta(t)} = (1+\dot{\zeta})[(K-1)\, u(\zeta, t) - K]. \tag{4}$$

Local equilibrium condition

$$u(\zeta, t) = 1 - (l/l_T)\, \zeta(t), \tag{5}$$

where the thermal length is defined by

$$l_T = |m\, \Delta C_0|/G, \tag{6}$$

with $m$ the liquidus slope and $G$ the thermal gradient.

Eqs. (1), (4) and (5) must be supplemented with the appropriate initial conditions. In what follows we will always study instantaneous jumps taking place at $t = 0$, in which the system has been sitting at rest in the thermal field long enough to homogenize the liquid concentration, so that:

$$C_L(\zeta, t=0) = C_\infty \quad (u(\zeta, 0) = 0), \tag{7a}$$

$$\zeta(t=0) = l_T/l. \tag{7b}$$

Note that, in actual experiments, a sudden jump of the pulling velocity always gives rise to a thermal transient [10]. In thin samples pulled at relatively modest velocities (of at most a few 10 $\mu$m/s), this transient is very short [11] with respect to those due to chemical diffusion, so that we neglect it here.

This free boundary one-sided problem can be recast into a closed integral equation for the front position. This reads (see appendix B of ref. [2] and appendix A of ref. [12]):

$$\begin{aligned}\mu^{-1}\zeta(t) &= 2\int_{\zeta(t_0)}^{\infty} dz\, [1-u(z, t_0)]\, G(\zeta(t), t \,|\, z, t_0) \\ &+ \int_{t_0}^{t} dt' \left\{ -2\left[1+\dot{\zeta}(t')\right]\left[1+\mu^{-1}K\zeta(t')\right] \right. \\ &\left. + \mu^{-1}\zeta(t')\left(1 + \frac{\zeta(t)-\zeta(t')}{t-t'}\right)\right\} \\ &\times G(\zeta(t), t \,|\, \zeta(t'), t'),\end{aligned} \tag{8}$$

where $G(\zeta(t), t \,|\, \zeta(t'), t')$ is the 1D diffusion Green function

$$G(z, t \,|\, z', t') = \frac{1}{\sqrt{4\pi(t-t')}} \exp\left(-\frac{(z-z'+t-t')^2}{4(t-t')}\right), \tag{9a}$$

and $\mu$, defined by

$$\mu = l_T/l, \tag{9b}$$

is the only dimensionless control parameter for the planar recoil problem. Note also that it can also be written

$$\mu = V/V_{MS}^{(0)}, \tag{9c}$$

where $V_{MS}^{(0)} = D/l_T$ is the small $G$ limit of the critical MS velocity in the thermal gradient $G$.

In the right-hand side of eq. (8), the first term describes the effect of the diffusion, for $t > t_0$, of the solute field which was present at the instant $t_0$ which has been singularized, while the second term accounts for the effects due to that part of the solute which is rejected on the front after $t_0$ (note that $t_0$ can be chosen at will, and does not have to be the time at which the velocity jump takes place). It is easily shown that, if we let $t_0 \to -\infty$, the first term vanishes, and eq. (8) reduces to the standard 1D form appropriate for stationary external constraints.

### 3. Initial and asymptotic regimes

Let us choose for $t_0$ in eq. (8) the instant of the velocity jump $t_0 = 0$. From eq. (4) one immediately gets $\dot{\zeta}(t=0) = -1$ (the system starts from rest). Using eqs. (7), one easily finds that the solution of eq. (8) can be expanded as:

$$\zeta(t) - \left[\zeta(0) + t\dot{\zeta}(0)\right] = t^{3/2} \sum_{n=0}^{\infty} c_n t^{n/2}. \quad (10a)$$

It is then found that, at short times,

$$\zeta(t) = \mu - t + \frac{4}{3\mu K\sqrt{\pi}} t^{3/2} - \frac{1}{2\mu^2 K^2} t^2 + O(t^{5/2}). \quad (10b)$$

In order to extract from eq. (8) the long-time asymptotic behavior of $\zeta(t)$, we now choose a value of $t_0$ large enough for a first order expansion in $\zeta(t)$ and in the departure

$$\delta u(z, t_0) = u(z, t_0) - \exp\{-[z - \zeta(t_0)]\} \quad (11)$$

of the concentration profile from the stationary one to be valid. The linearization of eq. (8) then yields:

$$\tfrac{1}{2}(1-\mu^{-1})\,\zeta(t) = \int_{t_0}^{t} dt' \left[\dot{\zeta}(t') + \frac{c}{2}\zeta(t')\right] \frac{\exp[-(t-t')/4]}{\sqrt{4\pi(t-t')}} + \tfrac{1}{2}\zeta(t_0)\,\mathrm{erfc}\left(\tfrac{1}{2}\sqrt{t-t_0}\right) + H(t-t_0 \mid t_0), \quad (12)$$

where

$$H(t-t_0 \mid t_0) = \int_0^{\infty} \frac{dz}{\sqrt{4\pi(t-t_0)}} \delta u(z, t_0) \times \exp\left[-\frac{(z-t+t_0)^2}{4(t-t_0)}\right], \quad (13)$$

$$c = 1 + \frac{2K-1}{\mu}. \quad (14)$$

Defining the Laplace transform

$$Z(s) = \int_{t_0}^{\infty} dt\, e^{-s(t-t_0)}\, \zeta(t), \quad (15)$$

we obtain from eq. (11):

$$Z(s) = \left(s + \frac{1-\mu}{\mu}\sqrt{s+\tfrac{1}{4}} + \frac{c}{2}\right)^{-1} \times \left[\zeta(t_0)\frac{\sqrt{4s+1}-1}{\sqrt{4s+1}+1} - \sqrt{4s+1}\, H(s \mid t_0)\right], \quad (16)$$

where $H(s \mid t_0)$ is the Laplace transform of expression (13). If one neglects the term proportional to $H$ in $Z(s)$, which accounts for the effect of $\delta u(z, t_0)$, $Z(s)$ can be inverted straightforwardly (a very similar calculation was performed in detail by Pohl in ref. [13]). However, we have no a priory knowledge of $\delta u(z \mid t_0)$: indeed, in any such solidification problem, initial conditions are specified by the value of $\zeta(t_0)$ and by the shape of the function $\delta u(z, t_0)$, which are independent quantities, only related by the fact that eq. (5) must be satisfied at $t = t_0$.

In the case which we study here, specifying $\delta u(z, t_0)$ would demand the knowledge of the full evolution between $t = 0$ and $t_0$. So, an exact calculation of the leading asymptotic behavior $\zeta_{as}(t)$ of $\zeta(t)$ is not possible.

However, it can be noticed that

$$\sqrt{s+\tfrac{1}{4}}\, H(s \mid t_0) = \tfrac{1}{2}\int_0^{\infty} dz\, \delta u(z, t_0) \exp\left[-\left(\sqrt{s+\tfrac{1}{4}} - \tfrac{1}{2}\right)z\right]. \quad (17)$$

On the other hand, decomposing the Laplace inverse of expression (16) into the pole(s) and cut contribution, one can check that, for large $(t - t_0)$,

$$\zeta_{as}(t) \approx Q_0(t)\, e^{-t/4} + \sum_i Q_i(t) \exp(s_i t), \quad (18)$$

where the $s_i$ are the poles (if any) of $Z(s)$ (eq. (16)), and $Q_0$ and $Q_i$ are constants or proportional to negative powers of $t$.

On the basis of the heuristic WL approximation [3], it seems plausible to assume that

$$u(z, t_0) = \left[1 - \mu^{-1}\zeta(t_0)\right] \times \exp\{-(1+\epsilon)[z - \zeta(t_0)]\},$$

with $\epsilon = O(\zeta(t_0))$, so that

$$\delta u(z) \approx \{-\mu^{-1}\zeta(t_0) - \epsilon[z - \zeta(t_0)]\} \times \exp\{-[z - \zeta(t_0)]\}.$$

Now, from eq. (17) it appears that any such exponentially decreasing profile does not give rise to any pole in the expression of $H(s \mid t_0)$, and that $\zeta_{as}(t)$ is given by expression (18), where

$$s_i = v_i^2 - \tfrac{1}{4}, \tag{19a}$$

and $v_i$ are the roots of

$$v_i^2 + (\mu^{-1} - 1)v_i + \tfrac{1}{2}c - \tfrac{1}{4} = 0, \tag{19b}$$

such that

$$\text{Re } v_i > 0. \tag{19c}$$

There may be 0, 1 or 2 such roots, depending on the values of $\mu$ and $K$. We then find that the final relaxation of $\zeta(t)$ is exponential, and the corresponding characteristic time $\tau$ is such that

$$\tau^{-1} = \text{Min}(\tfrac{1}{4}, \text{Re}\{-s_i\}). \tag{20}$$

The analysis of eq. (19b) then leads to the following results, where the various regions in the space of the control parameters $\mu = V/V_{MS}^{(0)}$ and $K$ are defined in fig. 2.

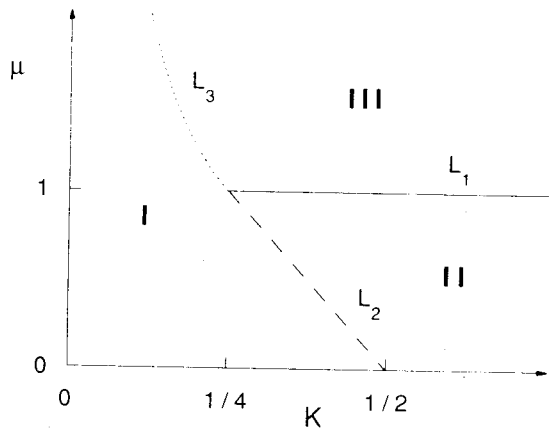


Fig. 2. Regions in the $(\mu, K)$ space for eqs. (21). The boundary lines are defined respectively by: $(L_1)$ $\mu = 1$, $K > \frac{1}{4}$; $(L_2)$ $\mu = 2 - 4K$, $\frac{1}{4} < K < \frac{1}{2}$; $(L_3)$ $\mu = 1/4K$, $K < \frac{1}{4}$.

Region I:

$$\zeta_{as}(t) \approx Q(t) \exp\left[-\left(\tfrac{1}{4} - v^2\right)t\right]. \tag{21a}$$

Region II:

$$\zeta_{as}(t) \approx Q(t) \exp\left(-\tfrac{1}{4}t\right). \tag{21b}$$

Region III:

$$\zeta_{as}(t) \approx Q(t) \exp\left[-\left(\tfrac{1}{4} - \text{Re } v^2\right)t\right] \times \sin\left[(\text{Im } v^2)t + \varphi\right], \tag{21c}$$

where the quantity $v$ appearing in eqs. (21a) and (21c) is given by

$$v = \tfrac{1}{2}\mu^{-1}\left(\mu - 1 + \sqrt{1 - 4K\mu}\right). \tag{21d}$$

Expressions (21) agree with the long time limits of previous asymptotic calculations [5,12]. In particular, in the small segregation coefficient limit ($K \ll 4V_{MS}^{(0)}/V$), the characteristic decay time is of order $D/KV^2$. Note that the larger $V$, the more narrow the range of validity of this result (which is often used by experimentalists for order of magnitude estimates).

Let us insist here on the two limitations of the above calculations:

(i) As already stated, we have had to make an ansatz about the shape of the departure of the u-profile from the stationary one.

(ii) Such a linear approximation cannot give any information about how close the front must have approached its stationary position $\zeta = 0$ for eqs. (21) to be relevant.

We will elucidate these two points in the next section, by comparing our asymptotic analysis to the results of the numerical integration of the full problem.

## 4. Numerical study

In order to perform a numerical integration of eq. (8), with initial conditions (7), we rewrite the integral of eq. (8) in terms of the integration variable $\sqrt{t - t_0}$ and then discretize the equation on the full $(0, t)$ time interval which we want to study. We then solve the resulting set of non-linear equations by means of a Newton–Raphson

method. We have checked, for each set of parameter values, that the relative changes of the results under doubling of the number of discretization steps were less than $10^{-3}$.

We have studied the recoil of the planar front for values of $\mu = V/V_{MS}^{(0)}$ ranging from 0.2 to 100, and for segregation coefficients $K = 0.1$, 0.2, 0.5 and 0.75. The values $K = 0.1$ and 0.75 were chosen because they correspond, respectively, to the well-studied succinonitrile–acetone [14,3] and $CBr_4$–$C_2Cl_6$ mixtures.

Fig. 3 exhibits the variation of the planar front position measured in units of the thermal length, $\hat{\zeta}(t) = \zeta(t)l/l_T = \tilde{\zeta}(t)/l_T$ (with $\tilde{\zeta}$ the position in physical units), versus the reduced time variable $t = \tilde{t}V^2/D$ (with $\tilde{t}$ the physical time), for $K = 0.75$. Fig. 4 illustrates, for $\mu = 2/3$, the dependence of $\hat{\zeta}(t)$ on the segregation coefficient.

We have compared these results with the predictions of the initial and asymptotic regime approximations. We find that, for all parameter values appropriate for jumps into the planar regime or not too far into the MS unstable region ($V \lesssim V_{MS}^{(0)}$), the short time expression (eq. (10b)) is valid only for times too short for the front recoil to be measurable with any accuracy.

Indeed, in order for experimental studies of jumps with $V \lesssim V_{MS}^{(0)}$ to be feasible without too much difficulty, $V_{MS}^{(0)}$ should be typically $\geq 1$ or a few $\mu$m/s. This means that $l_T$ should lie in the

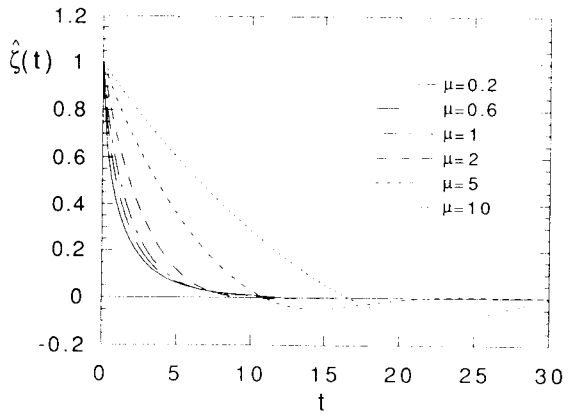


Fig. 3. Numerical results for the temporal evolution of the normalized front position $\hat{\zeta}(t) = \tilde{\zeta}(t)/l_T$ for constant $K = 0.75$ and several values of $\mu = V/V_{MS}^{(0)}$.

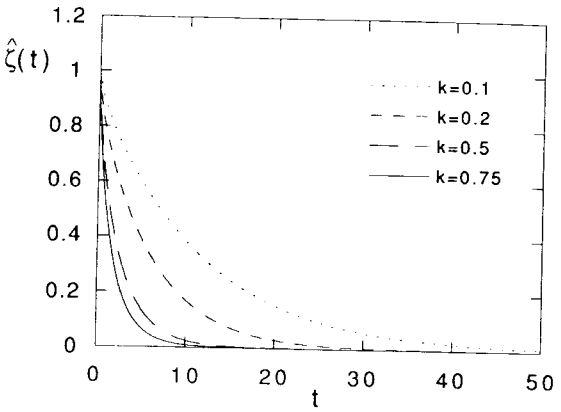


Fig. 4. Numerical results for the temporal evolution of the normalized front position $\hat{\zeta}(t)$ for constant $\mu = 2/3$ and several values of $K$.

range of a few hundred micrometers. Typical experimental resolutions for front positions are of the order of 1 $\mu$m. So, relative errors in $\tilde{\zeta}$ smaller than about $10^{-2}$ cannot be resolved.

Using this criterion, we find expression (10b) to be valid for reduced times of at most $10^{-1}$, at which the recoil of the front does not exceed $\sim 10^{-2} l_T$. So, the short time expansion – although it is useful to check the numerical results – is of no practical use for the analysis of the experimental data. This means in particular that the time regime where $\zeta(t) - \zeta(0) \approx -t$ should in general be too small to be observable. We have also compared our numerical results with the asymptotic expressions (21). For values of $\mu$ and $K$ lying in regions I and II of fig. 2, one finds indeed that, for large enough values of $t$, $q(t) = \dot{\zeta}(t)/\zeta(t)$ tends towards a constant which agrees with the predictions of eqs. (21a) and (21b). However, it appears that the time necessary to reach this limit increases with $K$. This is illustrated in fig. 5, where it is seen that, while for $\mu = 2/3$ and $K = 0.2$ (case 1), $q(t)$ has practically reached its asymptotic value of $-0.181$ for $t = 10$, when $\mu = 2/3$ and $K = 0.75$ (case 2), at time $t \approx 40$, $(q_{as} - q(t))/q_{as} \approx 15\%$. However, in this last case, the long time results for $|q(t)|$ do extrapolate to $\tau^{-1} = 1/4$. Note that, on the other hand, with our resolution criterion, the front will appear stationary when $\dot{\zeta}(t) \lesssim 10^{-2}$ i.e., respectively for $t \gtrsim 20$

(case 1) and $t \gtrsim 10$ (case 2). So, while these results prove that our ansatz about the asymptotic behavior $\zeta_{as}(t)$ is correct, it appears that experimental limitations should make this limit irrelevant in practice.

For values of $(\mu, K)$ in region III of parameter space, we do find (see fig. 3) that at large $t$, $\zeta$ oscillates about its stationary value in qualitative agreement with our asymptotic results. However, we have not been able – due to computation time limits – to perform the numerical integration up to large enough times for a comparison with eq. (21c) to be meaningful.

Two features which emerge from the results are worth of mention:
(i) The time $T$ necessary for "complete" recoil (i.e. for $|\hat{\zeta}| < 10^{-2}$), is noticeably larger, not only than the diffusion time $D/V^2$, but also than the "asymptotic time scale" $\tau$ (see eqs. (20) and (21)). For example, for $\mu = 2/3$ and $K = 0.2$, $T/\tau \sim 5$.
(ii) The characteristic recoil time scale, although it is not equal to the asymptotic one, increases with $K^{-1}$ in a roughly linear way.

Finally, we have compared our results with the predictions of the models proposed by Tiller et al. [5], Huang et al. [7] and Smith et al. [6]. In this last case, we have used the iterated value of the front position, as deduced from the Smith et al. concentration field, with the help of eq. (5). An example of such a comparison is shown in fig. 6. As expected from the brief discussion of their approximations made in section 1, none of these models is accurate at short and intermediate times. Analytical and numerical inspection shows that the model of ref. [6] is the only one which becomes valid in the asymptotic regime discussed above, and this only when $\mu \ll 1$.

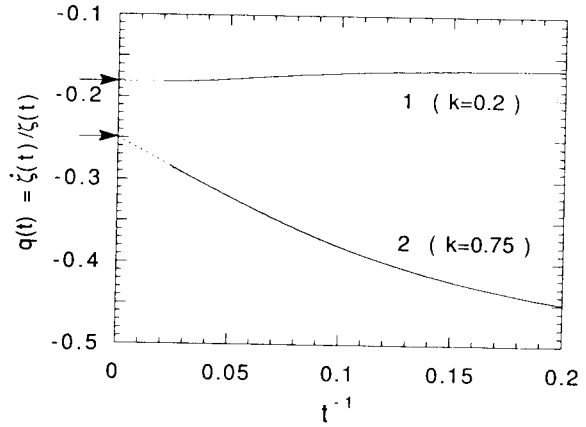


Fig. 5. Logarithmic slope $q(t) = \dot{\zeta}(t)/\zeta(t)$ versus inverse time for $\mu = 2/3$ and $K = 0.2$, 0.75. Solid lines: numerical results; dashed lines: extrapolations to $t^{-1} \to 0$; arrows: asymptotic predictions of eqs. (21).

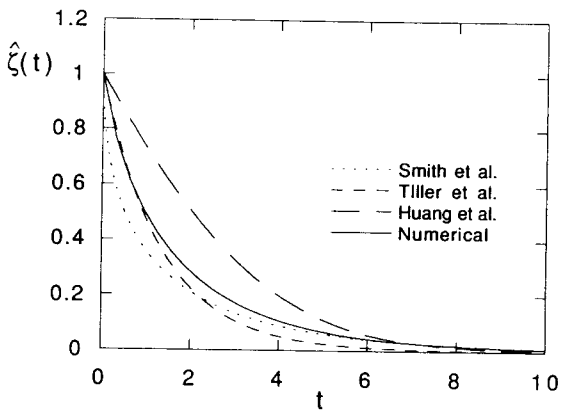


Fig. 6. Temporal evolution of the normalized front position $\hat{\zeta}(t)$ for $K = 0.75$ and $\mu = 2/3$. Dashed lines: predictions of Smith et al. [6], Tiller et al. [5], and Huang et al. [7]; solid line: numerical result. Note that the dotted curve is deduced from the concentration field calculated by Smith et al. with the help of eq. (5), i.e. is an iteration of their calculation.

## 5. Comparison with Warren–Langer approximation

The WL solution [3] relies, as already mentioned, on the assumption that the concentration profile is an exponential with a time-dependent range, i.e.:

$$u(z, t) = u(\zeta(t), t) \exp\left[-\frac{z - \zeta(t)}{L(t)}\right]. \qquad (22)$$

Calculating the zeroth-order moment of eq. (1) (by integrating it over the liquid volume) with the help of eqs. (4) and (22), they obtain:

$$-\left[1 + \dot{\zeta}(t)\right]\left[u(\zeta(t), t) - 1\right] = \frac{\mathrm{d}}{\mathrm{d}t}\left[L(t)\, u(\zeta(t), t)\right]. \qquad (23)$$

The planar recoil problem then reduces, with the help of eq. (5), to solving two non-linear differential equations:

$$1+\dot{\zeta}(t)=\frac{1}{L(t)}\left[1-\frac{\zeta(t)}{\mu}\right]\times\left[1+(K-1)\frac{\zeta(t)}{\mu}\right]^{-1}, \tag{24a}$$

$$\dot{L}(t)=L(t)\,\dot{\zeta}(t)\left[1-\frac{\zeta(t)}{\mu}\right]^{-1}+\frac{K\zeta(t)}{L(t)}\left[1+(K-1)\frac{\zeta(t)}{\mu}\right]^{-1}. \tag{24b}$$

The asymptotic relaxation of $\zeta(t)$ associated with eqs. (24) is easily calculated, and is found to agree with the results of the full analysis (eq. (18)) only in the limit $K \ll (1,(4\mu)^{-1})$. This is confirmed by direct comparison of our numerical results with numerical solutions of eqs. (24).

However, as discussed in section 4, this regime (as well as the initial one) is only of academic interest. We have therefore resorted to direct numerical comparisons, on the whole intermediate time interval relevant to experiments. Examples of such tests are shown in fig. 7. It is seen in fig. 7a that, for $\mu = 2/3$, the two graphs practically superpose: the difference $\Delta\zeta$ is at most $\approx 4\times10^{-3}$. This is typical of the quality of the agreement for velocity jumps with $V \lesssim V_{MS}$. Discrepancies are found to decrease to even lower levels when $K$ is decreased at constant $\mu$. For given $K$, the order of magnitude of $\Delta\zeta$ does not change noticeably when $\mu$ is increased to values larger than 1 – i.e. for jumps into the MS-unstable regime – as long as $\zeta$ relaxes monotonously.

For the parameters in region III of fig. 2, where $\zeta$ is found to exhibit, at large times, damped oscillations about its stationary value, it appears, as illustrated in fig. 7b, that the agreement becomes poorer as $\mu$ increases, but this only in the (late) oscillating regime. It always remains extremely good in the region of monotonous relaxation preceding the first zero of $\zeta$. Now, as will be discussed below in more detail, as it recedes the planar front accelerates so that it becomes

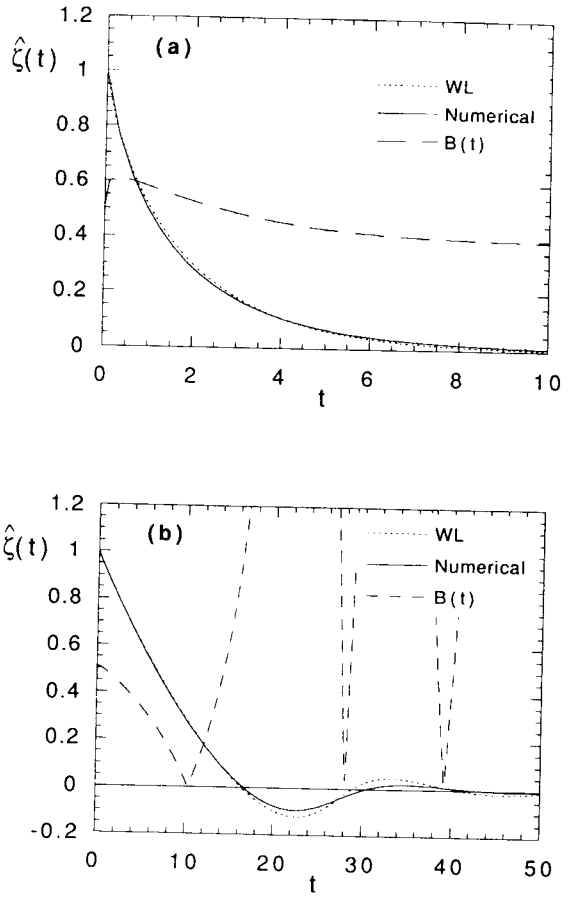


Fig. 7. Numerical test of the WL approximation. The solid and dotted lines correspond respectively to our numerical result and the integration of the WL differential equations (24) for the normalized front position $\hat{\zeta}(t)$; dashed line: function $B(t)$ of eq. (27). (a) $K = 0.75$, $\mu = 2/3$; (b) $K = 0.75$, $\mu = 10$.

MS-unstable much before this first zero is reached. So, the oscillating planar regime should never be observable. We therefore are led to conclude that the predictions of the WL approximation relevant to experiments are in all cases in excellent agreement with the predictions of the full theory.

In order to account for this result, we have tried to elaborate a criterion for the validity of the WL model. This criterion is based on the fact that eqs. (24) are obtained from the evaluation of the zeroth-order moment of the diffusion equa-

tion (1). We then calculate the first moment, i.e. we write

$$\int_{\zeta}^{\infty} \mathrm{d}z\ (z-\zeta)\left(\frac{\partial^2 u}{\partial z^2}+\frac{\partial u}{\partial z}\right)=\int_{\zeta}^{\infty} \mathrm{d}z\ (z-\zeta)\frac{\partial u}{\partial t}. \tag{25}$$

This can be rewritten, with the help of ansatz (22), as

$$\frac{\mathrm{d}}{\mathrm{d}t}[L(t)\ u(\zeta(t), t)] = -\left[1+\dot{\zeta}(t)\right]K[u(\zeta(t), t)-1]+M(t), \tag{26a}$$

where

$$M(t)=(-\dot{L}+L^{-1})\ u(\zeta, t) +(1+\dot{\zeta})\ [(K-1)\ u(\zeta, t)-K], \tag{26b}$$

which, when use is made of eq. (24a) together with (22), reduces to

$$M(t)=-\dot{L}(t)\ u(\zeta, t). \tag{26c}$$

Comparing eqs. (24) and (26a), it appears that a criterion for the validity of the exponential profile assumption is then provided by the condition

$$B(t)=\mu\left|\dot{L}u(\zeta, t)/L\dot{\zeta}\right| \ll 1. \tag{27}$$

Calculations of $B(t)$ for various values of $(K, \mu)$ show, as illustrated in fig. 7, that:
(i) in the regions (or in the cases) of monotonic decrease of $\zeta$, $B$ is typically of order 0.4 to 0.6.
(ii) our criterion of course loses its indicative value in the oscillating regimes, where $B$ exhibits divergences at the zeros of $\dot{\zeta}(t)$, since these are not in phase with those of $\dot{L}(t)$ [3].

From this, one could in principle only expect the WL approximation to be reasonably good. We have not been able to build any more sophisticated criterion which would permit to account, in a more precise way, for the remarkably good agreement at intermediate times which emerges empirically from the numerical analysis.

## 6. Cellular instability threshold

Let us now specialize to jumps from $V=0$ into the MS-unstable regime $V > V_{\mathrm{MS}}^{(0)}$. In such a case, it is clear that, for $t \to \infty$, the planar front is unstable against a cellular structure or periodic array of dendrites.

As time elapses after the jump, the planar front keeps accelerating so that, for $t > t_1(\mu, K)$, its velocity $v_{\mathrm{fr}} = V(1+\dot{\zeta})$ becomes larger than $V_{\mathrm{MS}}^{(0)}$. For $t = t_{1+}$ the transient concentration profile is a priori different from the stationary one corresponding to $V = V_{\mathrm{MS}}$. More precisely, the concentration gradient $G_{\mathrm{c}}$ ahead of the front, as given by eq. (4), is

$$\left|G_{\mathrm{c}}/G_{\mathrm{c}}^{\mathrm{MS}}\right|_{t=t_1} = 1-(1-K)\zeta/\mu, \tag{28}$$

where

$$G_{\mathrm{c}}^{\mathrm{MS}} = -\Delta C_0\ V_{\mathrm{MS}}/D \tag{29}$$

is the value corresponding to the MS threshold in the stationary state. As long as $(1-K)\zeta > 0$ (i.e., as long as the front is not in the oscillating regime, which we will find to be irrelevant below), $|G_{\mathrm{c}}(t_1)| < |G_{\mathrm{c}}^{\mathrm{MS}}|$. So, in this non-stationary situation the cellular instability will take place at some later time $t_{\mathrm{c}}$, with $v_{\mathrm{fr}}^{\mathrm{c}} > V_{\mathrm{MS}}^{(0)}$, and the wavelength of the first unstable deformation mode $\lambda_{\mathrm{c}}(\mu)$ will be different from the standard critical one, $\lambda_{\mathrm{MS}} \equiv \lambda_{\mathrm{c}}(1)$. This also entails that, for $V < V_{\mathrm{MS}}^{(0)}$, transient cellular instabilities are excluded.

In order to calculate $\lambda_{\mathrm{c}}(\mu)$, one must perform a linear stability analysis of the *transient* planar front state. Following Warren and Langer, we simplify this analysis by performing it in the adiabatic approximation – that is, in the calculation of the rate of amplification of fluctuations, we ignore the time dependence of $\zeta$ and $u$.

Setting

$$Z(x, t) = \zeta(t) + \delta\zeta\ \exp(\mathrm{i}kx+\omega t), \tag{30a}$$

$$U(x, z, t) = u(z, t) + \delta u\ \exp\{\mathrm{i}kx - q[z-\zeta(t)]+\omega t\}, \tag{30b}$$

where $\zeta(t)$ and $u(z, t)$ are the planar transient front position and concentration profile, and lin-

earizing eq. (4) as well as the Gibbs–Thompson equation

$$U(x, Z(x,t), t) = 1 - \frac{Z(x,t)}{\mu} - \frac{d_0}{l}\kappa(x), \tag{31}$$

with $\kappa(x)$ the front curvature and $d_0$ the capillary length [2], one obtains the dispersion equation:

$$\omega\left[1 - \frac{(1-K)\zeta}{\mu}\right] - K(1+\dot{\zeta})\, g_c(t) - \frac{\dot{\zeta}}{\mu} = \left[q + (1+\dot{\zeta})(K-1)\right] \times \left[-g_c(t) - \frac{1}{\mu} - \frac{d_0}{l}k^2\right], \tag{32}$$

where

$$g_c(t) = -(1+\dot{\zeta})\left[1 - \frac{\zeta}{\mu}(1-K)\right] \tag{33a}$$

is the reduced concentration gradient on the front,

$$q = \frac{1+\dot{\zeta}}{2} + \left[\frac{(1+\dot{\zeta})^2}{4} + \omega + k^2\right]^{1/2}, \tag{33b}$$

and

$$\zeta \equiv \zeta(t), \quad \dot{\zeta} \equiv \dot{\zeta}(t). \tag{33c}$$

We now look for the "transient cellular bifurcation" defined by Re $\omega = 0$, d(Re $\omega$)/d$k = 0$. Indeed, it can be proved (using the method described in ref. [15]) that this bifurcation is non-oscillating (i.e. that $\omega$ is real in the critical region).

We have studied eq. (32) numerically, using for $\zeta(t)$ the results of our numerical integration of the full front equation. The main result of this study is that, for jumps to $\mu$ values large enough for $\zeta(t)$ to exhibit oscillations, the cellular instability always occurs long before the first zero of $\zeta$ is reached. We can therefore immediately conclude, on the basis of the discussion in section 5, that the instability threshold can be accurately calculated with the help of the WL approximation for $\zeta(t)$. We have checked this directly for values of $\mu$ ranging from 1 to 100. We find, for example, that, for $\mu = 100$ and $K = 0.1$, the relative error in the time $t_c$ at which the instability occurs is $\Delta t_c/t_c \approx 0.14$, while that on the critical wavevector is $\Delta k_c/k_c \approx 3 \times 10^{-4}$. For $\mu = 1.2$ and $K = 0.1$, $\Delta t_c/t_c \approx 5 \times 10^{-3}$ and $\Delta k_c/k_c \approx 6 \times 10^{-2}$.

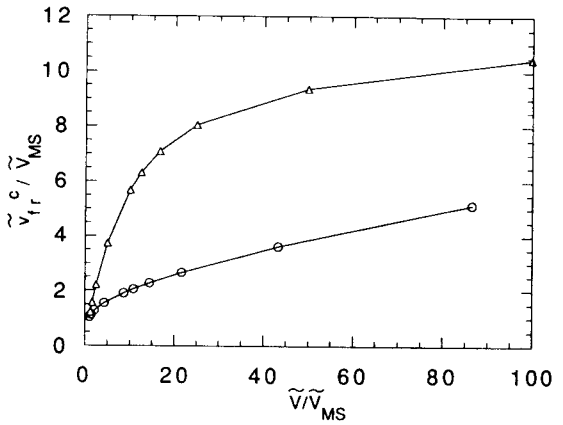


Fig. 8. Reduced front velocity at the cellular threshold, $v_{fr}^c / V_{MS}$, versus $V/V_{MS}$. Circles: alloy 4 mol% of $CBr_4$–$C_2Cl_6$ ($K = 0.75$, $G = 8\times10^3$ K/m, $d_0/l_T = 5.89\times10^{-4}$); triangles: alloy 5.5 mol% of succinonitrile–acetone ($K = 0.1$, $G = 6.7\times10^3$ K/m, $d_0/l_T = 3.63\times10^{-8}$); lines are given as a guide to the eye.

As could be expected, we find that the larger $\mu$, the larger the value of $v_{fr}^c/V_{MS}$ corresponding to the bifurcation (the larger the departure from

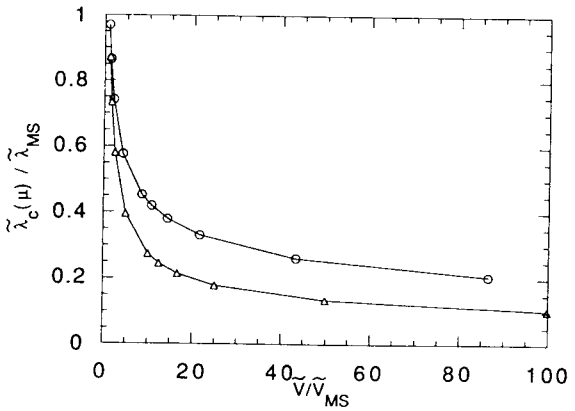


Fig. 9. Reduced wavelength of the first unstable mode $\tilde{\lambda}_c / \tilde{\lambda}_{MS}$ (in physical units) versus $V/V_{MS}$. Symbols and lines as defined in fig. 8.

the stationary configuration when $v_{Fr} = V_{MS}$). Two examples of this are shown in fig. 8. Note that, here, we use the actual value of $V_{MS}$, which differs from $V_{MS}^{(0)}$ by corrections $O((d_0/l_T)^{1/3})$. Also shown, in fig. 9, are the corresponding variations of $\tilde{\lambda}_c/\tilde{\lambda}_{MS}$, where $\tilde{\lambda}_{MS}$ and $\tilde{\lambda}_c$ are the values of the MS and critical wavelengths in physical units. It is seen that $\tilde{\lambda}_c/\tilde{\lambda}_{MS}$ is a decreasing function of $\mu$. Its behavior for $\mu \gg 1$ is easily understood: in this limit, the bifurcation occurs for times so small that $1 + \dot{\zeta} \ll 1$. Solving the bifurcation equations with $k_c \gg |1 + \dot{\zeta}|$ yields

$$k_c^3 = \left(\frac{2\pi l}{\tilde{\lambda}_c}\right)^3 \cong \frac{l}{2d_0}\left[K(1+\dot{\zeta})^2\left(1-(1-K)\frac{\zeta}{\mu}\right)-\frac{\dot{\zeta}}{\mu}\right] \cong \frac{l}{2d_0\mu}, \quad (34)$$

so that $\tilde{\lambda}_c \sim V^{-1/3}$. This explains the flattening of the $\tilde{\lambda}_c(\mu)$ curves found for, typically, $\mu \gtrsim 25$. When associated with the WL theory [3], this behavior suggests that most of the variations in dendritic spacings observed in the $\mu \gg 1$ regime should primarily result from the selection mechanism in the dendritic regime itself, rather than from initial instability effects.

## 7. Conclusion

The results of our study can be summarized rather simply:

(i) Neither the initial nor the asymptotic regimes for the recoil of the planar front – which can be characterized analytically – should be relevant to experimental studies. In particular, the short time expansion (10b) loses validity at times too short for accurate measurements to be possible. This should result in the fact – which should not be mistaken for in a deficiency of experimental conditions – that one will usually measure an apparent initial value of $\dot{\zeta}$ different from $-1$.

(ii) Direct numerical integration of the full front equation shows that the WL heuristic model provides, for all practical purposes, a very good approximation of the exact results. Indeed, the oscillating planar front recoil regime, where its accuracy becomes poorer, will never be observed, since it would always start after the cellular instability has already taken place. This same model can also confidently be used to calculate the threshold of this instability. This should make the detailed analysis of experimental data considerably easier, by avoiding the quite heavy task of solving the full dynamical problem.

## Acknowledgements

We are indebted to G. Faivre for several stimulating discussions. L.R.-P. acknowledges a grant and financial support (Pro. PB90-0030) from the Direccion General de Investigacion Cientifica y Técnica (Spain).

## References

[1] W.W. Mullins and R.F. Sekerka, J. Appl. Phys. 35 (1964) 444.
[2] See, for instance, B. Caroli, C. Caroli and B. Roulet, Instabilities of planar solidification fronts, in: Solids Far from Equilibrium, Ed. C. Godrèche (Cambridge University Press, Cambridge, 1992), and references therein.
[3] J.A. Warren and J.S. Langer, Predictions of dendritic spacings in a directional solidification experiment (preprint 1992).
[4] J.C. Clayton, M.C. Davidson, D.C. Gillies and S.L. Lehoczky, J. Crystal Growth 60 (1982) 374.
[5] W.A. Tiller, K.A. Jackson, J.W. Rutter and B. Chalmers, Acta Met. 1 (1953) 428.
[6] V.G. Smith, W.A. Tiller and J.W. Rutter, Can. J. Phys. 33 (1955) 723.
[7] W. Huang, Q. Wei and Y. Zhou, J. Crystal Growth 100 (1990) 26.
[8] B. Caroli, C. Caroli and B. Roulet, J. Crystal Growth 76 (1986) 31.
[9] J.C. Géminard, J. Bechhoefer and P. Oswald, J. Crystal Growth 114 (1991) 640.
[10] J.J. Favier, Thèse, Université de Grenoble (1977); J.J. Favier, J. Crystal Growth 49 (1980) 373.
[11] M.-M. Lebrun, Thèse, Université Paris 7 (1987).
[12] B. Caroli, C. Caroli and B. Roulet, J. Physique 48 (1987) 1623.
[13] R.G. Pohl, J. Appl. Phys. 25 (1954) 1170.
[14] R. Trivedi and K. Somboonsuk, Acta Met. 33 (1985) 1061.
[15] B. Caroli, C. Caroli and B. Roulet, J. Physique 43 (1982) 1767.